Journal of Energy Chemistry 47 (2020) 128–131

Contents lists available at ScienceDirect

Journal of Energy Chemistry

journal homepage: www.elsevier.com/locate/jechem

http://www.journals.elsevier.com/journal-of-energy-chemistry/

Letter

# The origin of sulfuryl-containing components in SEI from sulfate additives for stable cycling of ultrathin lithium metal anodes

Jin-Xiu Chen[a,b], Xue-Qiang Zhang[b], Bo-Quan Li[b], Xin-Meng Wang[b,c], Peng Shi[b], Wancheng Zhu[a,*], Aibing Chen[c], Zhehui Jin[d], Rong Xiang[e], Jia-Qi Huang[f,*], Qiang Zhang[b,*]

[a] Department of Chemical Engineering, Qufu Normal University, Qufu 273165, Shandong, China
[b] Beijing Key Laboratory of Green Chemical Reaction Engineering and Technology Department of Chemical Engineering, Tsinghua University, Beijing 100084, China
[c] College of Chemical and Pharmaceutical Engineering, Hebei University of Science and Technology, Shijiazhuang 050018, Hebei, China
[d] School of Mining and Petroleum Engineering, Department of Civil and Environmental Engineering, University of Alberta, Edmonton, AB T6G 1H9, Canada
[e] Department of Mechanical Engineering, The University of Tokyo, Tokyo 113-8656, Japan
[f] Advanced Research Institute of Multidisciplinary Science, Beijing Institute of Technology, Beijing 100081, China

ARTICLE INFO

*Article history:*
Received 24 October 2019
Revised 22 November 2019
Accepted 24 November 2019
Available online 2 December 2019

*Keywords:*
Ultrathin lithium anodes
Dendrites
Electrolyte additives
Solid electrolyte interphase
Lithium batteries

In the light of wireless and non-fossil society based on portable electronics, electric vehicles, and smart grids, secondary batteries with higher energy density, faster charge, and safer operation are pursued persistently [1]. Nowadays, commercial lithium (Li)-ion batteries have been practically applied in our daily life. However, the energy density of Li-ion batteries based on intercalation chemistry is approaching to the theoretical value due to the limited specific capacity of graphite anode (372 mA h $g^{-1}$) [2]. In order to further improve the energy density of secondary batteries, Li metal anode was revisited owing to its extremely high theoretical specific capacity (3860 mA h $g^{-1}$) and low reduction potential (−3.04 V vs. standard hydrogen electrode) [3]. Moreover, Li metal anode can be combined with different types of cathodes, such as intercalated cathodes (e.g., $LiFePO_4$ and $LiNi_{0.5}Co_{0.2}Mn_{0.3}O_2$ (NCM523)) and conversion cathodes (e.g., sulfur and oxygen) to construct various next-generation battery systems [4,5].

However, the practical applications of Li metal anode have been severely hindered by the growth of Li dendrites since 1950s, which induces short lifespan and even safety issues of Li metal batteries. The primary cause of the formation and growth of Li dendrites is the inhomogeneous solid electrolyte interphase (SEI), which is firstly named by Peled [6]. Li metal can react with almost all non-aqueous electrolytes due to intrinsically high reactivity [7]. The decomposition products of Li metal and electrolyte precipitate on Li surface randomly to constitute SEI. The heterogeneity of SEI induces varied spatial resistance for the transport of Li ions, finally generating Li dendrites. The growth of Li dendrites depletes electrolyte by cracking SEI and reduces the utilization of deposited Li, further deteriorating the performance of Li metal batteries [8]. Therefore, designing appropriate electrolyte formulations to construct homogenous SEI is an effective strategy to regulate Li deposition and suppress Li dendrites [9].

In terms of energy density and the complexity of technology processes, electrolyte formulations are highly expected to stabilize Li metal anode together with other potential solutions, such as three-dimensional hosts [10], artificial coating [11–13], desolvation kinetics regulation [14,15], and polymer or solid electrolytes [16]. Tremendous efforts have been devoted to developing electrolyte formulations for suppressing Li dendrites, such as fluoroethylene carbonate (FEC)-containing electrolytes [15,17], additives [18,19], and highly concentrated electrolytes [20,21]. Fluorinated SEI gen-

* Corresponding authors.
*E-mail addresses:* zhuwancheng@tsinghua.org.cn (W. Zhu), jqhuang@bit.edu.cn (J.-Q. Huang), zhang-qiang@mails.tsinghua.edu.cn (Q. Zhang).

https://doi.org/10.1016/j.jechem.2019.11.024

erated by FEC-containing electrolytes and highly concentrated electrolytes has exhibited enormous potential in suppressing Li dendrites and prolonging the lifespan of Li metal batteries [22]. Generally, thick Li metal (>200 μm) is employed to evaluate the electrochemical performance of electrolyte, which conceals the severe issues with ultrathin Li (<50 μm) under practical conditions, such as the rapid depletion of fresh Li and electrolyte and the severe volume expansion [5,23]. Aurbach and co-workers demonstrated that the lifespan of Li metal batteries with ultrathin Li anode (50 μm) and $LiNi_{0.6}Mn_{0.2}Co_{0.2}O_2$ (3.3 mA h $cm^{-2}$) cathode is approaching 90 cycles at 0.15 C with FEC as a co-solvent compared to 20 cycles with ethylene carbonate as a co-solvent [17]. The above lifespan cannot still meet the demand of practical applications. Therefore, emerging electrolyte formulations are highly required to further enhance the uniformity of Li deposition and improve the cycle life of Li metal batteries with ultrathin Li anode.

In this contribution, trimethylene sulfate (TMS) was employed as a fresh type of additives to generate a favorable SEI for uniform Li deposition and promote the applications of ultrathin Li anode. The effectiveness of TMS in regulating Li deposition and suppressing Li dendrites was verified in Li | Li symmetrical cells in electrolyte of 1.0 M lithium hexafluorophate ($LiPF_6$) dissolved in FEC/dimethyl carbonate (DMC). The cycling time of Li | Li cells with TMS additives is more than 1300 h at 0.5 mA $cm^{-2}$ with a capacity of 0.5 mA h $cm^{-2}$ compared with 600 h without additives. While applied in a Li metal battery with an ultrathin Li anode (33 μm), a high loading $LiNi_{0.5}Co_{0.2}Mn_{0.3}O_2$ (NCM523) cathode (2.5 mA h $cm^{-2}$), and lean electrolytes (7.7 g $A^{-1}$ $h^{-1}$), 130 cycles were achieved in Li | NCM523 batteries with TMS additives compared with 60 cycles without additives at 0.4 C. Cyclic voltammetry and X-ray photoelectron spectroscopy (XPS) were further employed to disclose the role of TMS in the formation of SEI. TMS additives decomposed before the reduction of FEC. Sulfuryl-containing components and $Li_2O$ generated in SEI with TMS additives, which can further improve the uniformity of Li deposition in fluorinated SEI.

The effect of TMS additives on regulating Li deposition and suppressing Li dendrites was firstly evaluated in Li | Li symmetrical cells. The electrolyte with FEC as a co-solvent (denoted as FEC/DMC electrolyte) has exhibited attractive performance in enhancing the uniformity of Li deposition. Therefore, TMS additives were introduced into FEC/DMC electrolyte to further prolong the cycle life of ultrathin Li anode. While TMS additives were employed, stable cycles with more than 1300 h was achieved in Li | Li cell without significant polarization increase at 0.5 mA $cm^{-2}$ with a capacity of 0.5 mA h $cm^{-2}$ (Fig. 1(a)). In contrast, only 600 h was obtained with a sharp polarization increase in electrolyte without TMS additives. The polarization voltage of batteries with TMS additives decreases from 60 to 42 mV after 700 h and then increases to 70 mV after 1300 h. However, the polarization voltage of batteries without TMS additives increases from 76 to 223 mV after 700 h (Fig. S2). The Li | Li cells with TMS additives also render low charge transfer resistance (Fig. S3). The increase of polarization is mainly induced by the formation and accumulation of dead Li and the depletion of electrolyte. The dendritic Li breaks from the root and generates easier in comparison to nodule-like Li [24]. The addition of TMS additives can suppress the formation of dead Li and maintain stable polarization voltage in long cycle life.

Scanning electron microscope (SEM) characterizations were further conducted in order to observe the morphology of Li deposition with and without TMS additives directly. Li | Li cells were disassembled after 5 and 50 cycles to obtain the cycled Li. The deposition morphology of Li with TMS additives is slightly smoother and more compact than that without additives after 5 cycles (Fig. 1(b) and (c)). The surface of Li anode presents compact morphology with TMS additives even after 50 cycles (Fig. 1(d)), differing from the porous and pulverized morphology of Li anode without TMS

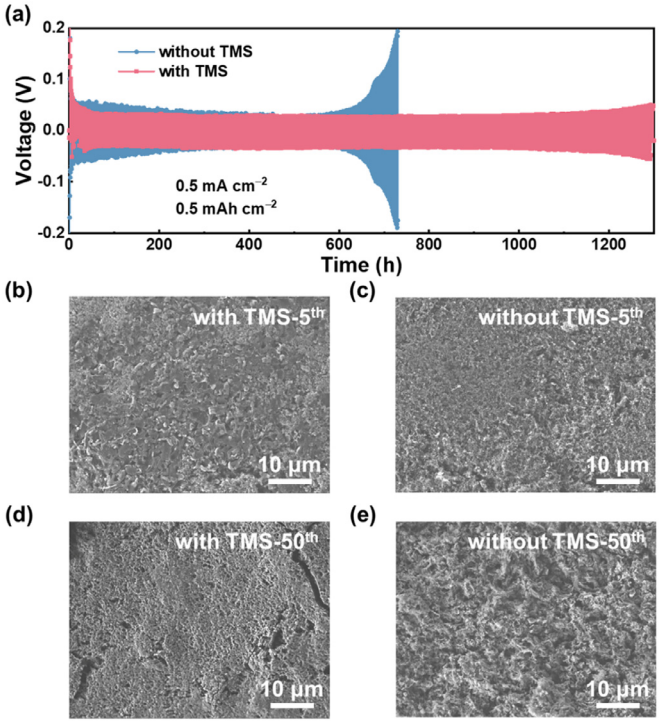


**Fig. 1.** Electrochemical performance of Li | Li symmetrical cells and SEM images of Li metal anodes after cycles with/without TMS additives. (a) Cycling performance of Li | Li symmetrical cells at 0.5 mA $cm^{-2}$ with a capacity of 0.5 mA h $cm^{-2}$. The deposition morphology of Li at the 5th cycle with (b) and without (c) TMS additives and at the 50th cycle with (d) and without (e) TMS additives.

additives evidently (Fig. 1(e)). The accumulation of dead Li was further disclosed from the cross-sectional view. The initial thickness of ultrathin Li anode is ca. 33 μm (Fig. S4a). After 35 cycles, the thickness of Li anode increases to 60 μm in the presence of TMS additives (Fig. S4b). Nevertheless, the thickness of Li anode expands to 91 μm without TMS additives (Fig. S4c). The formation and accumulation of dead Li induced by Li dendrites are significantly suppressed by TMS additives. TMS additives contribute to improving the uniformity of Li deposition, increasing the utilization of deposited Li per cycle, and suppressing the formation and accumulation of dead Li, which finally maintains stable polarization and prolongs the cycle life of Li | Li cells effectively.

In a practical Li metal battery, an ultrathin Li anode, a high loading cathode and lean electrolytes are necessary to achieve the goal of high energy density. NCM cathode based on intercalated mechanism has been commercialized successfully, such as NCM523 and NCM622. Coupling an ultrathin Li metal anode with a high loading NCM cathode emerges as a promising battery system with more than 350 W h $kg^{-1}$ at cell level. Li | NCM523 batteries were employed in this work to evaluate the effect of TMS additives. An ultrathin Li metal anode (33 μm, ca. 6.6 mA h $cm^{-2}$), a high loading NCM523 cathode (2.5 mA h $cm^{-2}$), and lean electrolyte (7.7 g $A^{-1}$ $h^{-1}$) were employed in a Li | NCM523 battery. The amount of electrolyte cannot be further decreased in 2032-type coin cells in order to confirm the wetting of cathode. The benchmark of the evaluation of performance is the 80% capacity retention of the initial capacity. Furthermore, the cycle life of a practical Li metal battery decreases with the rise of charge rate. In the presence of TMS additives, the capacity of Li | NCM523 batteries decreases to 80% retention after 130 cycles (Fig. 2(a)). On the contraty, Li | NCM523 batteries without TMS additives decay to 80% capacity retention after only 60 cycles. The polarization voltage of a battery without TMS additives increases sharply and

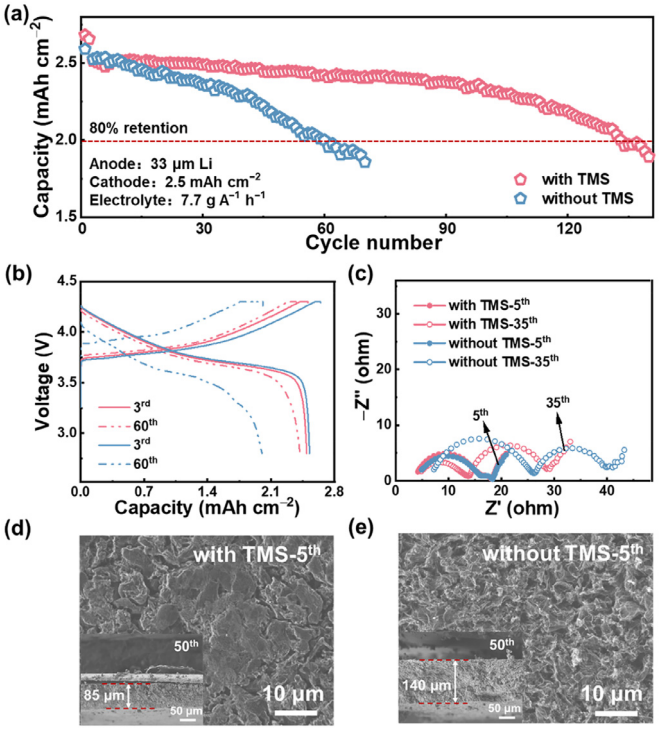


**Fig. 2.** The performance of TMS additives in Li | NCM523 batteries. (a) Cycling performance of Li | NCM523 batteries with and without TMS additives at 0.4 C after two formation cycles at 0.1 C. (b) The corresponding voltage profiles of Li | NCM523 batteries at the 3rd and 60th cycle. (c) EIS spectra of Li | NCM523 batteries. The deposition morphology of cycled Li anode with (d) and without (e) TMS additives at the 5th cycle. The insert images are the side view of Li anode after 50 cycles.

the capacity declines quickly within 60 cycles (Fig. 2(b)). The electrochemical impedance spectroscopy (EIS) was conducted to detect the evolution of internal resistance in Li | NCM523 batteries (Fig. 2(c)). The semicircle in high frequency can be assigned to the impedance of Li ions migration through the SEI on electrode surface, and the semicircle in low frequency represents the impedance of charge transfer. Obviously, the addition of TMS additives can decrease impedance for Li ions migration. The above results indicate that TMS additives afford to benefit the migration of Li ions in SEI.

The deposited Li with TMS additives at the 5th cycle is in the form of nodule with a diameter of 5 μm (Fig. 2(d)), the surface of which is smooth without obvious pulverization. In contrast, the deposited Li without TMS additives exhibits porous and crumpled morphology (Fig. 2(e)). The same results of the morphology of Li anode with and without TMS additives were obtained at the 50th cycle (Fig. S5a and b). After 50 cycles, the thickness of ultrathin Li anode with TMS additives increases from 33 μm to 85 μm, which is smaller than 140 μm obtained in electrolyte without TMS additives (Fig. 2(d) and (e)). The significant decrease in thickness of Li anode after cycles proves the effect of TMS additives in suppressing Li dendrites and inhibiting the accumulation of dead Li. The huge volume expansion of Li metal anode is still a great challenge for stable practical Li metal batteries, appealing more efforts to handle this issue.

In order to further demonstrate how TMS additives protect Li metal anode, cyclic voltammetry (CV) test was conducted to obtain the reduction potential of electrolyte (Fig. S6). TMS decomposes before FEC, illustrating that TMS additives participate in the formation of SEI prior to FEC. X-ray photoelectron spectroscopy (XPS) was performed to disclose the components of SEI. In Li 1*s* spectra (Fig. 3(a)), the ratio between the content of $Li_2O$ and LiF increases in presence of TMS additives. $Li_2O$ and LiF play the critical

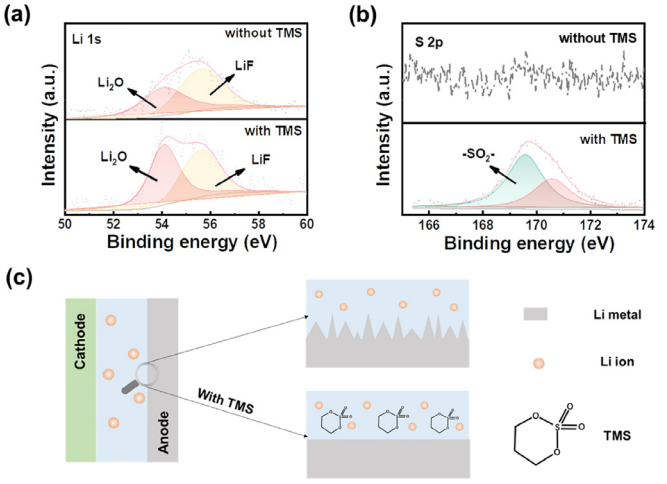


**Fig. 3.** XPS spectra of the SEI on ultrathin Li anode in Li | NCM523 batteries after 5 cycles. (a) Li 1*s* and (b) S 2*p*. (c) The schematics of the role of TMS additives in protecting ultrathin Li anode.

role in enhancing the uniformity of Li deposition. In S 2*p* spectra (Fig. 3(b)), there is no signal of S on Li surface without TMS additives. In presence of TMS additives, there is a peak of $-SO_2-$ from sulfuryl-containing components, which indicates that TMS additives decompose and participate in the formation of SEI. Sulfuryl-containing components and increased content of $Li_2O$ generated in SEI with TMS additives [15,25]. TMS additives participate into the formation of SEI composed of sulfuryl-containing components and increased content of $Li_2O$, which contributes to suppressing Li dendrites, improving the utilization efficiency of Li per cycle, and inhibiting the accumulation of dead Li (Fig. 3(c)).

In conclusion, trimethylene sulfate (TMS) was developed as a new type of additives in this work to regulate Li deposition and promote the applications of ultrathin Li anode. TMS additives decompose before FEC to enhance the uniformity of Li deposition. Thus, sulfuryl-containing components and increased content of $Li_2O$ were introduced into fluorinated SEI, further improving the homogeneity of SEI and promoting more uniform Li deposition than that only in fluorinated SEI. While TMS additives were applied in a Li metal battery with an ultrathin Li anode (33 μm), a high loading $LiNi_{0.5}Co_{0.2}Mn_{0.3}O_2$ (NCM523) cathode (2.5 mA h cm$^{-2}$), and lean electrolyte (7.7 g A$^{-1}$ h$^{-1}$), 130 cycles were achieved in Li | NCM523 batteries with TMS additives compared with 60 cycles without additives. This work not only proposes a new type of additives to suppress Li dendrites but also provides guidance for the design of electrolyte formulations to stabilize ultrathin Li anode in practical batteries.

## Declaration of Competing Interest

None.

## Acknowledgments

This work was supported by the National Key Research and Development Program (2016YFA0202500 and 2016YFA0200102), the National Natural Science Foundation of China (21676160, 21825501, and U1801257), and Tsinghua University Initiative Scientific Research Program.

## Supplementary materials

Supplementary material associated with this article can be found, in the online version, at doi:10.1016/j.jechem.2019.11.024.

## References


[1] Y. Liang, C.Z. Zhao, H. Yuan, Y. Chen, W. Zhang, J.Q. Huang, D. Yu, Y. Liu, M.M. Titirici, Y.L. Chueh, H. Yu, Q. Zhang, InfoMat 1 (2019) 6–32.
[2] M. Li, J. Lu, Z. Chen, K. Amine, Adv. Mater. 30 (2018) 1800561.
[3] X. Shen, H. Liu, X.B. Cheng, C. Yan, J.Q. Huang, Energy Storage Mater. 12 (2018) 161–175.
[4] X.Q. Zhang, C.Z. Zhao, J.Q. Huang, Q. Zhang, Engineering 4 (2018) 831–847.
[5] J. Liu, Z.N. Bao, Y. Cui, E.J. Dufek, J.B. Goodenough, P. Khalifah, Q.Y. Li, B.Y. Liaw, P. Liu, A. Manthiram, Y.S. Meng, V.R. Subramanian, M.F. Toney, V.V. Viswanathan, M.S. Whittingham, J. Xiao, W. Xu, J.H. Yang, X.Q. Yang, J.G. Zhang, Nat. Energy 4 (2019) 180–186.
[6] E. Peled, J. Electrochem. Soc. 126 (1979) 2047–2051.
[7] X.Q. Zhang, X.B. Cheng, Q. Zhang, Adv. Mater. Interfaces 5 (2018) 1701097.
[8] M.D. Tikekar, S. Choudhury, Z.Y. Tu, L.A. Archer, Nat. Energy 1 (2016) 16114.
[9] X. Xu, S. Wang, H. Wang, C. Hu, Y. Jin, J. Liu, H. Yan, J. Energy Chem. 27 (2018) 513–527.
[10] X. Shen, X. Cheng, P. Shi, J. Huang, X. Zhang, C. Yan, T. Li, Q. Zhang, J. Energy Chem. 37 (2019) 29–34.
[11] N.W. Li, Y.X. Yin, C.P. Yang, Y.G. Guo, Adv. Mater. 28 (2016) 1853–1858.
[12] R. Xu, Y. Xiao, R. Zhang, X.B. Cheng, C.Z. Zhao, X.Q. Zhang, C. Yan, Q. Zhang, J.Q. Huang, Adv. Mater. 31 (2019) 1808392.
[13] Y.X. Yuan, F. Wu, G.H. Chen, Y. Bai, C. Wu, J. Energy Chem. 37 (2019) 197–203.
[14] H. Yang, L. Yin, H. Shi, K. He, H.-M. Cheng, F. Li, Chem. Commun. 55 (2019) 13211–13214.
[15] X.Q. Zhang, X. Chen, X.B. Cheng, B.Q. Li, X. Shen, C. Yan, J.Q. Huang, Q. Zhang, Angew. Chem. Int. Ed. 57 (2018) 5301–5305 *Angew. Chem.* 130 (2018)5399–5403.
[16] M. Zhu, J. Wu, Y. Wang, M. Song, L. Long, S.H. Siyal, X. Yang, G. Sui, J. Energy Chem. 37 (2019) 126–142.
[17] E. Markevich, G. Salitra, F. Chesneau, M. Schmidt, D. Aurbach, ACS Energy Lett. 2 (2017) 1321–1326.
[18] Y. Lu, Z. Tu, L.A. Archer, Nat. Mater. 13 (2014) 961–969.
[19] Y.L. Ma, Z.X. Zhou, C.J. Li, L. Wang, Y. Wang, X.Q. Cheng, P.J. Zuo, C.Y. Du, H. Huo, Y.Z. Gao, G.P. Yin, Energy Storage Mater. 11 (2018) 197–204.
[20] X.L. Fan, L. Chen, X. Ji, T. Deng, S.Y. Hou, J. Chen, J. Zheng, F. Wang, J.J. Jiang, K. Xu, C.S. Wang, Chem 4 (2018) 174–185.
[21] S. Chen, J. Zheng, D. Mei, K.S. Han, M.H. Engelhard, W. Zhao, W. Xu, J. Liu, J.G. Zhang, Adv. Mater. 30 (2018) 1706102.
[22] X.Q. Zhang, X.B. Cheng, X. Chen, C. Yan, Q. Zhang, Adv. Funct. Mater. 27 (2017) 1605989.
[23] X.B. Cheng, C. Yan, J.Q. Huang, P. Li, L. Zhu, L.D. Zhao, Y.Y. Zhang, W.C. Zhu, S.T. Yang, Q. Zhang, Energy Storage Mater. 6 (2017) 18–25.
[24] Y. Li, W. Huang, Y. Li, A. Pei, D.T. Boyle, Y. Cui, Joule 2 (2018) 2167–2177.
[25] Y. He, X. Ren, Y. Xu, M.H. Engelhard, X. Li, J. Xiao, J. Liu, J.-G. Zhang, W. Xu, C. Wang, Nat. Nanotechnol. 14 (2019) 1042–1047.